JOURNAL OF PROPULSION AND POWER
Vol. 11, No. 5, September–October 1995

Crack Growth Resistance Due to Shot Peening in Carburized Gears

Katsumi Inoue* and Masana Kato†
Tohoku University, Sendai 980, Japan

This article deals with the effect of shot peening on crack growth in carburized gears. Since residual stress plays an important role in this analysis, an evaluation of the residual stress induced in a carburized gear tooth due to shot peening is presented first. It has been proposed on the basis of the assumption that the residual stress is caused by the difference of volume expansion between the case and the core, and the influence of both the reduction of retained austenite and the strain caused by shot peening are considered. The shot peening is fairly effective to the reduction of fatigue crack growth rate. The resistance to crack growth is demonstrated by the simulation of crack propagation in both the carburized gear and the shot-peened gear.

Introduction

THE high load capacity of carburized gears originates from the existence of hardened layer and residual stress. This is the main reason that the carburization is recommended as the normal heat treatment for aircraft gears in the AGMA standard.[1] The authors have made clear the effects of hardness and residual stress on the enhancement of bending fatigue strength, and proposed an experimental formula for the evaluation of strength.[2-4] The effectiveness of the proposed formula has been verified by the comparison with many fatigue test results, including the results for AISI 9310 carburized gears.[5]

The shot peening improves the strength of carburized gears still more, because it increases the hardness and residual stress in the surface layer. On the other hand, the shot peening as well as the carburization reduces the ductility of the material, and generally, the harder the material is, the faster the fatigue crack propagates. The crack propagation problem in such carburized and surface-treated gears is considerably complicated to solve because of the metallographic inhomogeneity and the distribution of residual stress that characterize the treatments. Honda and Conway[6] and Ahmad and Loo[7] calculated the stress intensity factor for a gear tooth and predicted the direction of the crack propagation. However, the influence of residual stress and metallographic inhomogeneity were not discussed in their reports. The authors have simulated the fatigue crack growth in a carburized gear tooth including the effect of residual stress,[8-10] and discussed the fracture mechanics based strength evaluation.[11-13] However, the crack growth for shot-peened gears has not been solved yet, because the residual stress distribution in the tooth has remained unsolved.

Recently, the authors[14] proposed a practical method for the estimation of the residual stress in a carburized and shot-peened gear tooth by considering the influence of martensitic transformation of retained austenite and the strain induced in the surface layer. Using this method as a basis, the crack growth in a shot-peened gear tooth is analyzed in this article. The method for residual stress estimation is briefly reviewed first, then the effect of shot peening on the resistance to the fatigue crack growth is discussed. The critical crack length is calculated from the threshold stress intensity factor to demonstrate the influence of shot peening on the initiation of crack growth. The crack propagation in both the carburized gear and the shot-peened gear is simulated.

Shot Peening to Carburized Gears

The carburized test gears are prepared to confirm the effect of shot peening. The gears have the same dimensions as those used for the fatigue tests,[2-4] i.e., module = 5, number of gear teeth = 18, face width = 8 mm. The gear blanks are made of the low alloy steel SCM415, and copper-plated about 20 μm thick to prevent the gear sides from carburizing. The plating makes the longitudinal characteristics of the gears approximately uniform. Then the gears are hobbed and gas-carburized to have the effective case depth d_{eff} (depth to 550 Hv) of about 0.9 mm.

The shot diameter, the measurement of shot peening intensity, etc., are prescribed in the SAE standard.[15] The shot-peening treatment is prescribed by the arc height and the coverage, and they are measured by an Almen strip. The full coverage is recommended for most machine parts. However, the gears are frequently peened three times the exposure time for full coverage, which is confirmed by the Almen strip, because the shots are hard to peen the tooth fillet owing to the shape of gears. The authors have found that the condition of 0.5–0.6 mm arc height and 300% coverage is most adequate

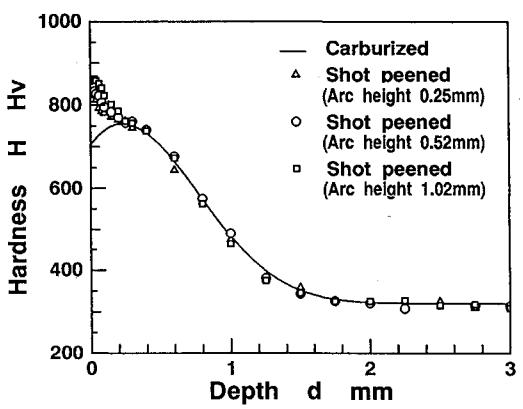

Fig. 1 Hardness distribution in the test gears.

Received April 7, 1994; presented as Paper 94-2935 at the AIAA/ASME/SAE/ASEE 30th Joint Propulsion Conference and Exhibit, Indianapolis, IN, June 27–29, 1994; revision received Oct. 17, 1994; accepted for publication Oct. 24, 1994. Copyright © 1994 by the American Institute of Aeronautics and Astronautics, Inc. All rights reserved.

*Associate Professor, Department of Machine Intelligence and Systems Engineering, Aramaki-Aoba, Aoba-ku. Member AIAA.
†Professor, Department of Machine Intelligence and Systems Engineering.

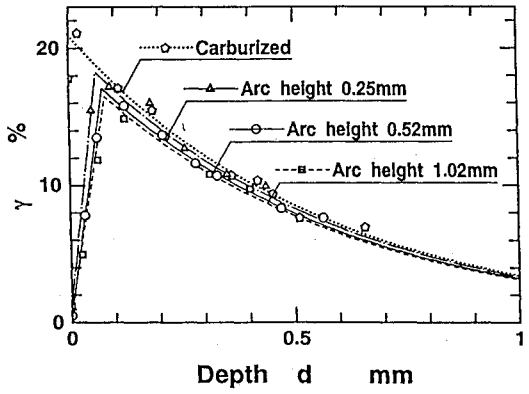

Fig. 2 Reduction of the retained austenite by shot peening.

for the enhancement of bending strength of carburized gears.[5] Referring to this, the carburized test gears are shot peened under the condition of 300% coverage and 0.25, 0.52, or 1.02 mm arc height.

The hardness distributions at the tooth fillet are shown in Fig. 1. As carburized, the hardness decreases towards the surface mainly due to the nonmartensitic layer. The surface hardness is about 160 Hv increased by shot peening and the effect reaches to the depth of about 0.2 mm. This depth is not very influenced by the shot-peening intensity. The retained austenite, which is measured by x-ray diffraction method, is reduced as shown in Fig. 2. In case of carburized gears, the maximum amount of retained austenite is measured at the surface, and it is about 21%. It is transformed to martensite by shot peening, and the retained austenite at the surface is diminished. The distribution of retained austenite $\gamma(\%)$ after shot peening is expressed by the following equation:

$$\gamma = \begin{cases} \gamma_m \cdot d/d_m & d \le d_m \\ \gamma_m \exp\left(-2.30 \dfrac{d - d_m}{1.5 d_{\text{eff}}}\right) & d > d_m \end{cases} \quad (1)$$

where γ_m, % and d_m, mm are the amount and the depth of the maximum retained austenite. The distributions obtained by Eq. (1) are shown by the lines in the figure.

The fatigue tests are performed to clarify the effect of shot peening on the strength and lives. The test procedure is shown in the previous reports[2-5] and it is omitted in this article. The test is terminated at $N = 3 \times 10^6$. Obtained fatigue strengths are 761 and 1176 MPa for the carburized gear and the shot-peened gear of 0.52 mm arc height, respectively. As previously reported,[3-5] the fatigue strength σ_u (MPa) is estimated from the core hardness H_c (Hv), the surface hardness H_s (Hv), and the surface residual stress σ_R (MPa) as follows:

$$\sigma_u = \sigma_{uc} + \sigma_{usc} + \sigma_{uR} = 1.17H_c + 257 + 3.1 \exp[0.0097(H_s - H_c)] - 0.5\sigma_R \quad (2)$$

where σ_{uc} (MPa) shows the fatigue strength of noncarburized gears, σ_{usc} and σ_{uR} (MPa) indicate the increase of strength due to hardened layer and residual stress, respectively.

Evaluation of Strain Caused by Shot Peening

The shot peening also causes a permanent strain at the tooth surface, and it is needed for the evaluation of the residual stress. For the exact analysis, the strain should be calculated by solving the impact problem, taking into consideration of the shakedown of material, the rebound of shots, etc. However, it is very complicated. In this section, therefore, an approximate strain is evaluated from the arc height of an Almen strip instead.

Strain Evaluated from Almen Strip

The dimensions of Almen strip A are indicated in Fig. 3. To measure the shot intensity, the strip is fixed to the holder by using screws, then one surface is shot-peened. It is assumed here that a compressive permanent strain is induced by shot peening as illustrated in Fig. 4. Let the strain be ε_0 at the surface, and its distribution be linear from the surface to the depth δ. If the strip deflects spherically after losing the screws, the radius of curvature ρ is obtained from the arc height h, which is defined by the central deflection from the datum points A to D:

$$\rho = (1/2h)[(l_1/2)^2 + (l_2/2)^2 + h^2] \quad (3)$$

With the deflection, the bending strain $-z/\rho$ and the linear strain ε_F are assumed to be generated in the strip. Summing these strains, the strain is given as follows:

$$\varepsilon_x = \begin{cases} \varepsilon_F - \dfrac{z}{\rho} - \dfrac{\varepsilon_0}{\delta}\left(-z - \dfrac{t}{2} + \delta\right) & z \le -\dfrac{t}{2} + \delta \\ \varepsilon_F - \dfrac{z}{\rho} & z \ge -\dfrac{t}{2} + \delta \end{cases} \quad (4)$$

$$\varepsilon_y = \varepsilon_x$$

The stress–strain relation is derived by assuming $\sigma_z = 0$, which is normally used in the thin plate theory, and the stresses are obtained by substituting the strains ε_x and ε_y obtained from Eq. (4). The bending moment is then obtained from the stresses, and it is equalized to zero to evaluate the strain ε_0. The relation between the strain and the radius of curvature is finally derived as follows:

$$\varepsilon_0\rho(-3\delta t + 2\delta^2) + t^3 = 0 \quad (5)$$

In this research, the depth δ is assumed to be equal to the thickness of layer in which the hardness is increased by shot peening. Figure 5 shows the hardness distribution in the Almen strips used for the confirmation of arc height. The depth δ is not very influenced by the shot intensity, and it is about

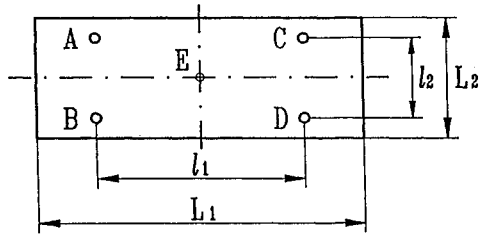

L_1= 76.20 mm l_1 = 31.75 mm t = 1.30 mm
L_2= 19.05 mm l_2 = 15.88 mm

Fig. 3 Dimensions of the Almen strip A.

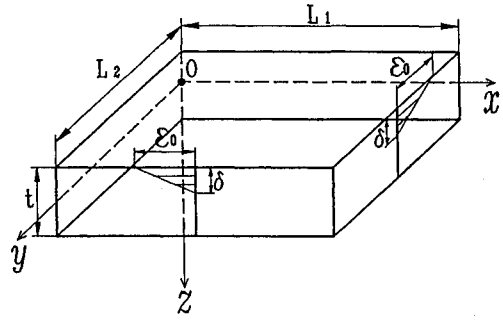

Fig. 4 Compressive strain induced in the Almen strip by shot peening.

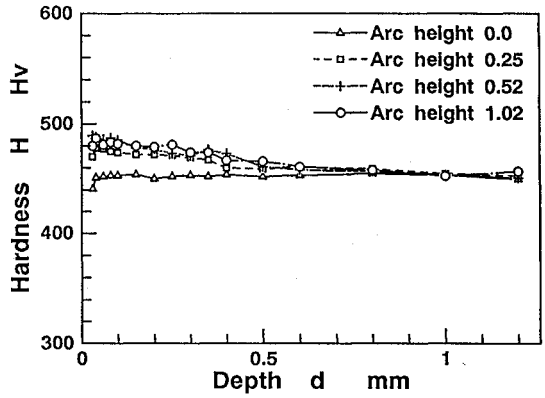

Fig. 5 Hardness distribution in the Almen strip.

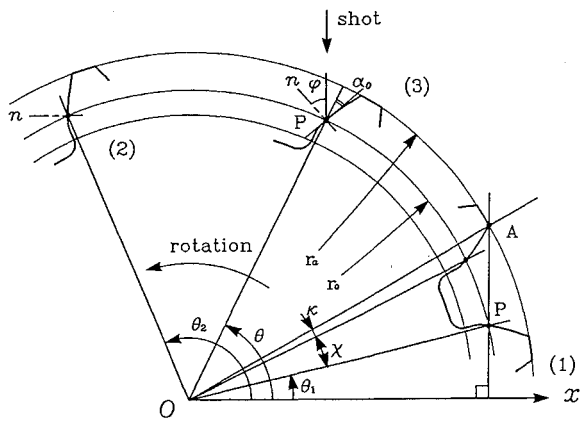

Fig. 6 Variation of the shot stream direction to gear tooth.

0.9 mm for all shot-peening conditions selected in this research.

Influence of Shot Obliquity to Tooth Surface

Since the gear is slowly rotated during shot-peening treatment, the direction of shot stream to tooth surfaces varies as schematically shown in Fig. 6. If the pitch point P is taken as a reference, a tooth is peened between the position (1), where the adjacent tooth tip blocks the shot stream, and the position (2), where the tooth surface is parallel to the stream. These positions are indicated by the angles θ_1 and θ_2, respectively, of which origin is the radial line x normal to the shot stream. The angles θ_1 and θ_2, and the average of angle φ, which is the angle between the stream and the tooth normal [Fig. 6 (3)], are expressed as follows:

$$\theta_1 = \tan^{-1}\left[\cot(\chi + \kappa) - \frac{r_0}{r_a \sin(\chi + \kappa)}\right]$$

$$\theta_2 = \alpha_0 + \frac{\pi}{2}$$

$$\hat{\varphi} \equiv \frac{1}{\theta_2 - \theta_1}\int_{\theta_1}^{\theta_2} \varphi \, d\theta = \frac{1}{\theta_2 - \theta_1}\int_{\theta_1}^{\theta_2} (\theta - \alpha_0)\, d\theta \tag{6}$$

$$= \frac{1}{2}(\theta_1 + \theta_2) - \alpha_0$$

where r_0 is the pitch radius, r_a is the tip radius, and α_0 is the standard pressure angle; and the angle χ and κ are given by

$$\chi = \pi/z$$

$$\kappa = \text{inv}\,\alpha_a - \text{inv}\,\alpha_0 \tag{7}$$

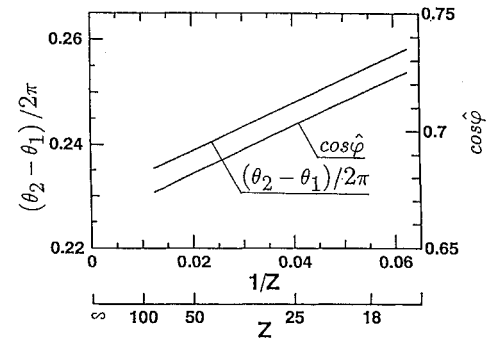

Fig. 7 Diagram for the estimation of exposure and impact angle (cf. Fig. 6).

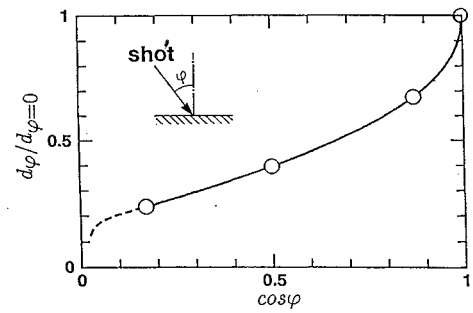

Fig. 8 Effect of shot obliquity on the hardened depth.

In the preceding expressions, z and α_a are number of gear teeth and pressure angle at the tip, respectively, and the function inv α is defined as inv $\alpha = \tan\alpha - \alpha$. $(\theta_2 - \theta_1)/2\pi$ and $\cos\hat{\varphi}$ obtained from Eq. (6) are indicated in Fig. 7 as a function of the number of gear teeth for standard spur gear. The former is about 0.25, and this shows that every tooth is peened for a quarter of the process time.

Meguid and Duxbury[16] made an experiment to clarify the influence of shot obliquity. For various impact angle φ of S170 shot stream, they measured the depth d_φ where the hardness increased. The ratio of d_φ to $d_{\varphi=0}$, which is the depth obtained from the normally peened test piece, is shown in Fig. 8. Figures 7 and 8 suggest that the shot-peening intensity confirmed by the Almen strip has to be reduced to some extent to estimate the effect of shot peening for the gear tooth. Indeed, the ratio $d_\varphi/d_{\varphi=0}$ for gear tooth is approximately 0.5, since $\cos\varphi$ is about 0.7 as shown in Fig. 7. Therefore, it is assumed in this research that the arc height h is modified as expressed in Eq. (8), and h_G is used for the evaluation of the strain at the tooth surface:

$$h_G = h \cdot \left(\frac{\theta_2 - \theta_1}{2\pi} \times \frac{C}{100}\right) \cdot \frac{d_\varphi}{d_{\varphi=0}} \tag{8}$$

In the expression, C (%) is the coverage and $C = 300\%$ is usually selected for the gears as described previously. The term in parentheses indicates the exposure time for the tooth surface, and it is taken as unity if a greater value is obtained in Eq. (8), since the intensity is determined so that the arc height is approximately saturated at the full coverage. From the above considerations, the strain ε_0 for the gear tooth is evaluated by substituing h_G for h in Eqs. (3–5).

Computation of Residual Stress

A computer program is developed based on the idea described in the above section. The flow of computation is shown in Fig. 9. The left half of the flow is for the carburized gears.[17] This evaluation was based on the assumption that the residual stress was caused by the volume difference between the case

and the core of tooth due to the martensitic transformation in cooling. To estimate the carbon content from the hardness, an experimental formula has been presented.[17] The specific volume, which is expressed as a function of carbon content, is calculated considering the influence of retained austenite. The strain is then estimated from the volume expansion due to the change of specific volume, and the residual stress is computed as the two-dimensional initial strain problem by the finite element method.

The right half of the flow is added to modify the amount of retained austenite and to evaluate the strain in the surface layer for shot-peened gears. As previously shown in Fig. 1, the hardness of carburized gears increases by the depth of about 0.2 mm, therefore, the evaluated surface strain is assumed to decrease linearly to this depth. And this strain is superposed on the strain caused by the volume expansion. The mesh and the boundary conditions for the finite element analysis are shown in Fig. 10. It is modeled by using 2988 linear triangular elements. Many fine elements are lined normal to the fillet such that they form a crack and the calculated stresses are used for the evaluation of stress intensity factor in the next section.

The residual stress in the gear tooth for $h = 0.52$ mm and $C = 300\%$ is computed by the proposed method. The stress distribution along a line normal to the fillet is shown by the broken line (shot-peened 1) in Fig. 11. The stress is increased greatly in the layer to the depth of 0.2 mm as compared with the stress distribution for carburized gear. The latter is obtained by neglecting the reduction of retained austenite and the surface strain, and it is represented by the dash and dot line. The calculated residual stress is close to the stress measured by an X-ray method, though it is overestimated at the surface. The discrepancy may be mainly caused by the neglect of plasticity, however, the consideration of the plasticity complicates the analysis and it is contrary to the objective of this research. Another cause might be that the estimated surface strain ε_0 is excess for the carburized gears with hardened layer. The stress indicated by the solid line (shot-peened 2) is obtained by giving the surface strain of $\varepsilon_0/2$, and this is closer to the measured value. The stresses for $h = 0.25$ and 1.02 mm are also examined, and it is concluded that the proposed method can be used for the approximate estimation of the residual stress of carburized and shot-peened gears by reducing to half the surface strain evaluated in the previous section.

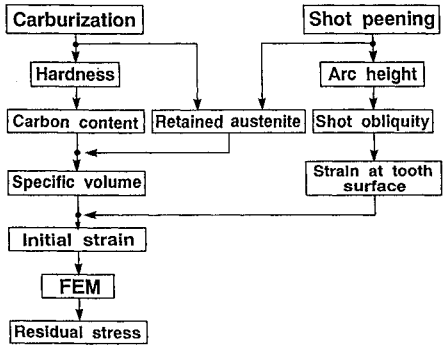

Fig. 9 Flow of the residual stress computation.

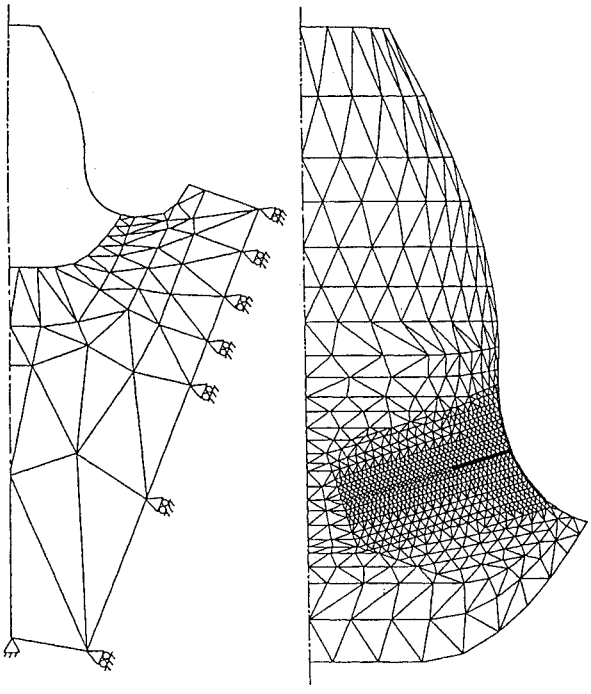

Fig. 10 Pattern of mesh and boundary conditions in the finite element analysis.

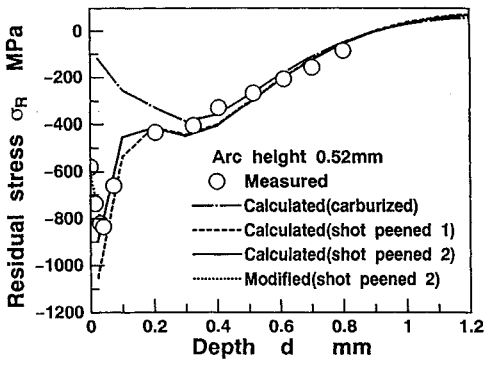

Fig. 11 Comparison of the estimated residual stress with the measured stress by X-ray method.

Resistance to Fatigue Crack Growth

Stress Intensity Factor

The narrow face width and the copper plating on the gear sides make the longitudinal characteristics of the test gears approximately uniform. In fact, the crack fronts observed in the fractured surfaces are almost linear. Therefore, two-dimensional fracture mechanics can be applied to this gear tooth. The stress intensity factor K_I for mode I is calculated by the influence function method[18,19] as follows:

$$K_I = \int_0^a f(x, a, \text{geometry})\sigma_y(x)\, dx \tag{9}$$

where $\sigma_y(x)$ is the sum of the bending stress and the residual stress for uncracked tooth, and it is evaluated at the position of crack, perpendicular to the crack. The influence function f for the case of plane strain is represented by the following expression:

$$f = \frac{1}{2}\left(\frac{1 - \nu}{E}\frac{\partial U}{\partial a}\right)^{-1/2}\frac{\partial w}{\partial a} \tag{10}$$

In this expression, U is the strain energy of the tooth with the crack a for an arbitrary load, and w is the crack opening displacement. E and ν are the modulus of elasticity and Poisson's ratio, respectively. The derivatives are numerically evaluated by the forward differences.

The stress intensity factor for the shot-peened gear of $h = 0.52$ mm is calculated and compared with the carburized gear as well as the gear without residual stress in Fig. 12. To consider the effect of residual stress precisely, the computed stress is slightly modified to fit the measured stress at the surface

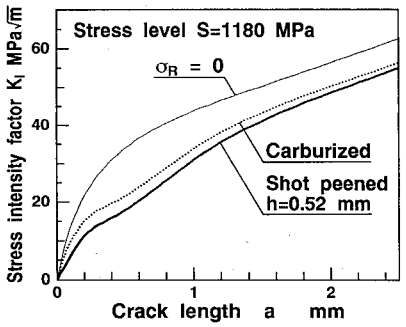

Fig. 12 Effect of residual stress on the stress intensity factor (tip loading).

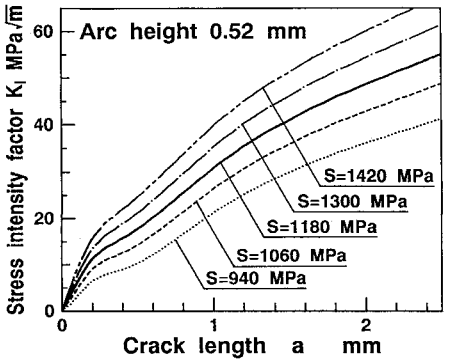

Fig. 13 Stress intensity factor for the shot-peened gear.

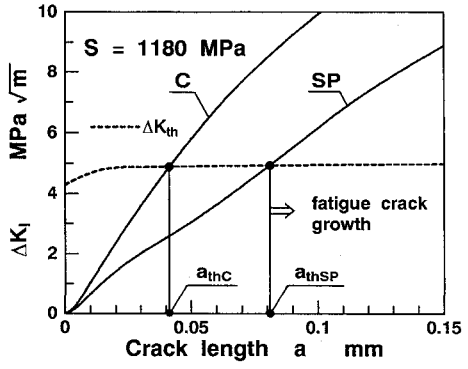

Fig. 14 Evaluation of the threshold length of crack a_{th}.

as shown by the dotted line (shot-peened 2) in Fig. 11, and it is used in this calculation. The fillet stress of an uncracked tooth is used to express the loading condition, and it is shown as the stress level S in the figure. The stress level 1180 MPa is slightly higher than the bending fatigue strength of the shot-peened test gear. It is clear that the stress intensity factor is considerably decreased by the residual stress. Figure 13 shows the stress intensity factors for the shot-peened gear for various stress levels.

Critical Crack Length for Propagation

The stress intensity factors in Fig. 12 are magnified and shown in Fig. 14. The ordinate indicates the stress intensity factor range for the pulsating load. The threshold stress intensity factor range ΔK_{th} is calculated from the hardness distribution of carburized gear[9,12,13] and it is illustrated by the broken line in the figure. It is assumed here that ΔK_{th} is not affected by the increase in hardness due to shot peening. Therefore, only one line is drawn for both the carburized gear and the shot-peened gear. The crack length a_{th} is determined from the intersection of these lines, and it is called the threshold length of crack in this article. Even if a crack exists at the tooth fillet, if the crack is shorter than a_{th}, the crack does not propagate naturally. In other words, the longer threshold length of crack means the higher bending strength. The threshold length is increased about 40 μm by shot peening in this case.

In Eq. (2), the higher strength is estimated by the higher surface hardness or higher compressive residual stress. If the hardness is increased, the threshold stress intensity factor K_{th} increases.[9,12,13] The higher compressive residual stress reduces the stress intensity factor as described in the above section. In either case, therefore, the longer threshold length of crack is obtained and the higher strength is also expected from this point of view, although the coefficients in Eq. (2) are not determined.

The threshold lengths are calculated for various stress levels and they are shown in Fig. 15. The hatched area under the line of a_{thSP} indicates the area of crack nonpropagation for the shot-peened gears. The increase of a_{th} is caused by the residual stress induced by shot peening, and it is marked in the region of low stress level.

Figure 16 shows the critical threshold length corresponding to the fatigue strength. The fatigue strength for the carburized gear and the shot-peened gear are plotted on the abscissa, and the intersections with the lines of a_{th} give the critical length a_{0C} and a_{0SP}. It is called the endurance length of crack in this article. It is clear from the definition that the endurance length is almost equal to the initial crack length corresponding to the fatigue strength, if it is estimated by assuming the whole life to the tooth breakage is the process of crack propagation. Obtained endurance lengths are about 80 and 96 μm. They are considerably longer than the length obtained previously.[11-13] The neglection of the stress intensity factor for mode II may cause the difference, however, it remains unsolved. Since the endurance length is obtained from the fatigue strength, it is represented by a function of material, heat treatment, and surface condition. Therefore, it might be used for the precise discussion of the strength based on fracture mechanics.

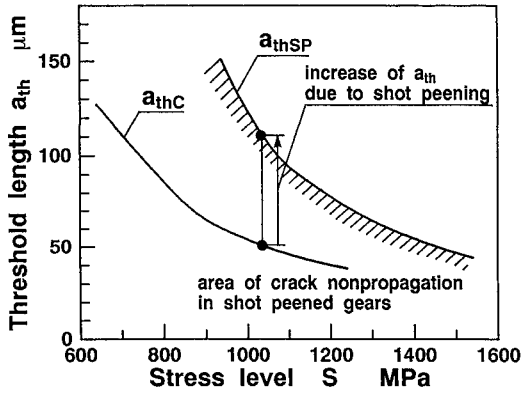

Fig. 15 Increase of the threshold length due to shot peening.

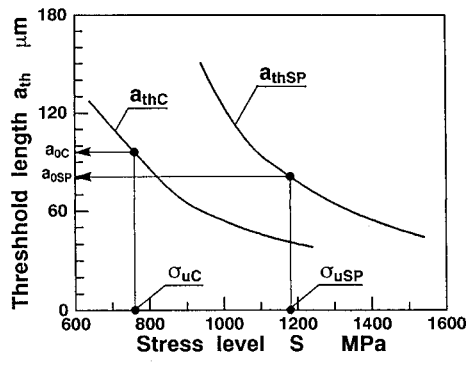

Fig. 16 Evaluation of the endurance length of crack a_0.

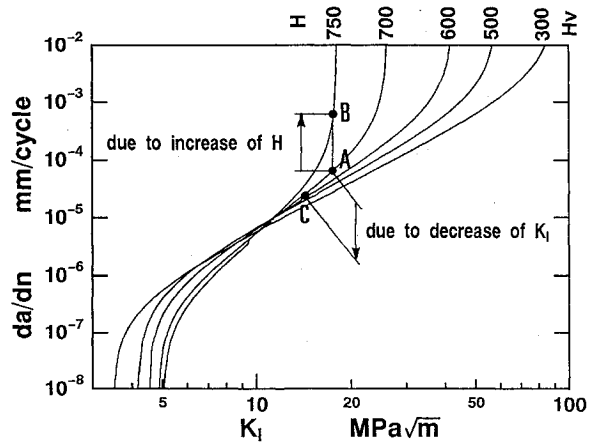

Fig. 17 Variation of the fatigue crack growth rate due to the increase of hardness and the decrease of stress intensity factor.

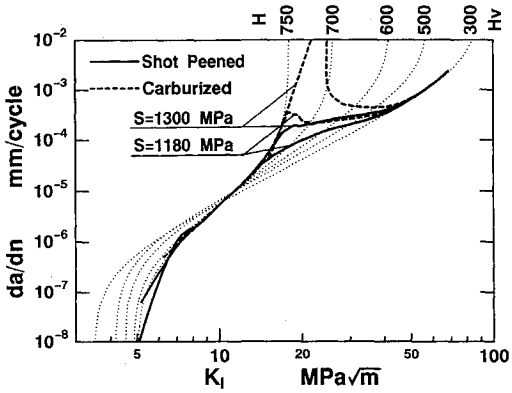

Fig. 18 Estimated fatigue crack growth rates for the test gears.

Crack Growth Rate and Residual Life

The crack growth rates in a steel have been expressed as a function of hardness.[9,12,13] They are illustrated in Fig. 17. A crack, which is represented by the point A, is supposed. Namely, the hardness at the crack tip is 700 Hv, and it is stressed to have the stress intensity factor of the point A. If the hardness of material is increased to 750 Hv, the condition of the crack shifts to the point B, and the fatigue crack growth rate d*a*/d*n* increases as shown in the figure. This indicates that the harder the material, the faster the crack propagates. On the other hand, the condition may shift to the point C along the line of 700 Hv if the stress intensity factor is reduced by, e.g., the residual stress. The decrease of crack growth rate is also shown in the figure.

When the crack length a is given at the tooth fillet of test gear, the hardness at the crack tip is obtained from the hardness of carburized gears shown in Fig. 1. The hardness increase due to shot peening is not used because the effect of stress hardening on the crack growth is not cleared. The fatigue crack growth rates d*a*/d*N*, which are similarly estimated from the hardness as described above, are plotted against the stress intensity factor in Fig. 18. In case of S = 1300 MPa, the crack growth rate of the carburized gear becomes fairly high at the subsurface, and it reduces to a moderate value after the crack propagates about 0.1 mm. Such a high rate is not observed in the shot-peened gear, because the residual stress reduces the stress intensity factor and it represses the rate. The crack growth rate of the carburized gear for S = 1180 MPa is still higher than the shot-peened gear, although a fairly high rate does not appear.

The crack growth is simulated for the test gears and the results are shown in Fig. 19. In this simulation, the existence of an initial crack, which is slightly longer than the threshold

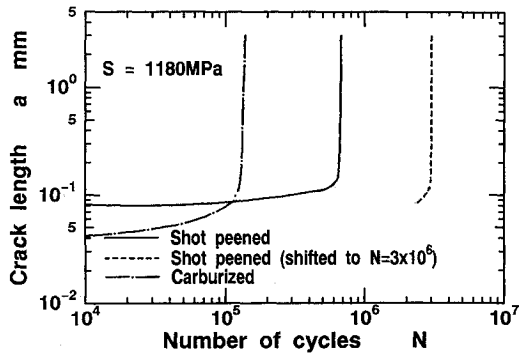

Fig. 19 Simulation of crack growth in the gear tooth.

length of crack, is assumed and the crack growth is calculated stepwise. The life of a carburized gear is rather longer than the life obtained by the fatigue test. The neglect of the stress intensity factor of mode II may lead to the longer life, however, it remains unsolved. Even so, this figure clearly demonstrates that the shot peening is fairly effective to reduce the crack growth and it leads to longer fatigue life. The crack growth represented by the broken line is obtained by the shift of the solid line to $N = 3 \times 10^6$, because the stress level is approximately equal to the fatigue strength of the gear and the fatigue test has been terminated at $N = 3 \times 10^6$. This suggests the residual life after crack propagation is about one-third of the fatigue life.

Conclusions

The crack growth in a shot-peened gear tooth was analyzed in this article. As the basis of the analysis, the residual stress was evaluated by the practical method that had been proposed by the authors. It was based on the assumption that the residual stress was caused by the difference of volume expansion in the case and the core, and the influence of the reduction of retained austenite and the strain in the surface layer induced by shot peening were considered. The conclusions may be summarized as follows:

1) The stress intensity factor for the shot-peened gear was rather small as compared with the factor for the carburized gear because of the effect of residual stress.

2) The proposed method was utilized for the estimation of the threshold length of crack and the endurance length of crack. By using these crack lengths, the effect of shot peening on the resistance to crack growth was discussed.

3) The fatigue crack growth rates for the shot-peened gear were calculated and presented. As compared with the rate for the carburized gear, the rate was considerably reduced by the residual stress.

4) The fatigue crack growth and the residual life of the shot-peened gear were simulated, and the effect of shot peening on the resistance to crack propagation was demonstrated quantitatively.

Acknowledgments

The carburization and shot peening of test gears were treated by Dowa Mining Corporation and Toyota Motor Corporation. The authors appreciate their kindness. The authors also express their thanks to Sung-ki Lyu and Gang Deng of Tohoku University for their valuable contributions to the stress measurement and the calculation of stress intensity factor.

References

[1]AGMA Standard 246.02A, "Practice for Carburized Aerospace Gearing," American Gear Manufacturers Association, 1983.

[2]Tobe, T., Kato, M., Inoue, K., Takatsu, N., and Morita, I., "Bending Strength of Carburized SCM420H Spur Gear Teeth," *Bulletin of the Japan Society of Mechanical Engineers*, Vol. 29, 1986, pp. 273–280.

[3]Inoue, K., Maehara, T., Yamanaka, M., and Kato, M., "The Effect of Shot Peening on the Strength of Carburized Spur Gear Teeth," *Japan Society of Mechanical Engineers International Journal, Ser III*, Vol. 32, 1989, pp. 448–454.

[4]Inoue, K., Kato, M., and Yamanaka, M., "Fatigue Strength and Crack Growth of Carburized and Shot Peened Spur Gears," *Proceedings of the 1989 International Power Transmission and Gearing Conference* (Chicago, IL), American Society of Mechanical Engineers, Vol. 2, 1989, pp. 663–668.

[5]Inoue, K., and Kato, M., "Estimation of Fatigue Strength Enhancement for Carburized and Shot-Peened Gears," *Journal of Propulsion and Power*, Vol. 10, No. 3, 1994, pp. 362–368.

[6]Honda, H., and Conway, J. C., "An Analysis by Finite Element Techniques of the Effects of a Crack in the Gear Tooth Fillet and Its Applicability to Evaluating Strength of the Flawed Gears," *Bulletin of the Japan Society of Mechanical Engineers*, Vol. 22, 1979, pp. 1848–1855.

[7]Ahmad, J., and Loo, F. T., "On the Use of Strain Energy Density Fracture Criterion in the Design of Gears Using Finite Element Method," *Proceedings of the 2nd International Power Transmission and Gearing Conference* (Chicago, IL), American Society of Mechanical Engineers, 1977, pp. 1–8 (77-DET-158).

[8]Inoue, K., Deng, G., and Kato, M., "Evaluation of the Strength of Carburized Spur Gear Teeth Based on Fracture Mechanics, 1st Report: Stress Intensity Factor Considering the Effect of Residual Stress Distribution in the Case," *Transactions of the Japan Society of Mechanical Engineers*, Vol. 55, C, 1989, pp. 1488–1493 (in Japanese).

[9]Deng, G., Inoue, K., Takatsu, N., and Kato, M., "Evaluation of the Strength of Carburized Spur Gear Teeth Based on Fracture Mechanics, 2nd Report: Characteristics of Crack Growth Rate in the Carburized Layer," *Transactions of the Japan Society of Mechanical Engineers*, Vol. 57, C, 1991, pp. 903–908 (in Japanese).

[10]Deng, G., Inoue, K., Takatsu, N., and Kato, M., "Evaluation of the Strength of Carburized Spur Gear Teeth Based on Fracture Mechanics, 3rd Report: The Crack Growth in Carburized Gear," *Transactions of the Japan Society of Mechanical Engineers*, Vol. 57, C, 1991, pp. 909–913 (in Japanese).

[11]Kato, M., Deng, G., Inoue, K., and Takatsu, N., "Evaluation of the Strength of Carburized Spur Gear Teeth Based on Fracture Mechanics, 4th Report: Proposal of a Method for Evaluating the Bending Strength Based on the Fatigue Crack Growth Characteristics," *Transactions of the Japan Society of Mechanical Engineers*, Vol. 57, C, 1991, pp. 2996–3001 (in Japanese).

[12]Inoue, K., Kato, M., Deng, G., and Takatsu, N., "Fracture Mechanics Based Evaluation of Strength of Carburized Gear Teeth," *Proceedings of the International Conference on Motion and Power Transmissions* (Hiroshima), Japan Society of Mechanical Engineers, 1991, pp. 801–806.

[13]Kato, M., Deng, G., Inoue, K., and Takatsu, N., "Evaluation of the Strength of Carburized Spur Gear Teeth Based on Fracture Mechanics," *Japan Society of Mechanical Engineers International Journal*, Vol. 36, C, 1993, pp. 233–240.

[14]Inoue, K., Lyu, S., Deng, G., and Kato, M., "Estimation of Residual Stress Due to Shot Peening in Carburized Gears and Its Effect on the Stress Intensity Factor," *Transactions of the Japan Society of Mechanical Engineers*, Vol. 60, C, 1994, pp. 3504–3509 (in Japanese).

[15]"SAE Standard, Test Strip, Holder and Gage for Shot Peening," Society for Automotive Engineers J442, 1968; "Procedures for Using Standard Shot Peening Test Strip," Society of Automotive Engineers J443, 1968; "Cast Shot and Grit for Peening and Cleaning," Society of Automotive Engineers J444, 1969.

[16]Meguid, S. A., and Duxbury, J. K., "A Practical Approach to Forming and Strengthening of Metallic Components Using Impact Treatment," *Proceedings of the 1st International Conference on Shot Peening* (Paris), Pergamon, 1981, pp. 217–228.

[17]Tobe, T., Kato, M., and Inoue, K., "A Method Estimating Residual Stresses from Hardness Distribution in View of Fatigue Strength of Carburized Gear Teeth," *International Journal of Vehicle Design, IAVD Congress on Vehicle Design and Components*, Vol. D, 1985, pp. D18,1–D18,18.

[18]Rice, J. R., "Some Remarks on Elastic Crack-Tip Stress Fields," *International Journal of Solids Structures*, Vol. 8, 1972, pp. 751–758.

[19]Besuner, P. M., "Residual Life Estimates for Structures with Partial Thickness Cracks," *Mechanics of Crack Growth*, American Society for Testing and Materials STP590, 1976, pp. 403–419.